Research Article

Thermal Stability and Tribological Behaviors of Tri-fillers Reinforced Epoxy Hybrid Composites

Tottyeapalayam Palanisamy Sathishkumar* and Palanisamy Navaneethakrishnan
Department of Mechanical Engineeirng, Kongu Engineering College, Erode, Tamilnadu, India

Ponnuswamy Maheskumar
Department of Mechanical Engineeirng, Nandha College of Engineering, Erode, Tamilnadu, India

* Corresponding author. E-mail: tpsathish@kongu.ac.in DOI: 10.14416/j.asep.2021.08.002
Received: 17 April 2021; Revised: 2 June 2021; Accepted: 10 June 2021; Published online: 4 August 2021

Abstract
The present works investigates the thermal stability and wear behaviour of tri-fillers reinforced hybrid composites. The Silica (S), Coconut shell (C) and Graphite (G) fillers reinforced homogeneous and functional graded epoxy composites are prepared by vertical injection molding techniques. The effect of filler contents, design parameters and its interaction on wear and friction behavior of SCG composites has been investigated. With help of Taguchi's techniques, L27 orthogonal array, a series of experiments are planned and conducted on pin-on-disc tribo machine with three different loading of 10, 20 and 30 N, three sliding velocities of 1, 1.5 and 2 m/s by varying the G filler content of 10, 20 and 30 wt% with constant weight fraction of S and C fillers of 10 wt%. The results shows that the increasing the Gr content was increased the wear resistance and rate. The optimization techniques used to determine the composites parameters.

Keywords: Epoxy, Graphite, Coconut shell powder

1 Introduction

Fiber reinforced epoxy composite (FRC) have found huge range of utility on various structural materials for aerospace, automobile, aviation and chemical industries because of their inert in good chemical resistant, thermal stability, mechanical properties, and electric insulation properties. In the area of tribology, polymer matrix composites had been slowly replacing traditional due to because of less weight-to-strength ratio, self-lubricant assets, low thermal coefficient of expansion, low wear rate and friction coefficient. The improvement of various characteristics of FRC have been improved by incorporating the various fillers which can be better bonding between matrix and fillers. Increase wear resistance of FRC was addition of various fillers and reinforcements whish were in different sizes, shapes, orientations and contents. The tribological behaviour of thermoplastic and thermosetting polymer composites were improved by incorporating inorganic fillers like ZrO_2, TiO_2, ZnO and Ti_3SiC_2 [1]–[7]. The micro and nano filler predominantly enhanced the wear rate of composite but different wear mechanism was occurred on the worn-out surface [8]. Incorporation of Silicon dioxide (SiO_2) in epoxy composites was increased the wear resistance [9], [10] but the reduced the mechanical strength and hardness of composite [11]. The post curing of SiO_2 filled epoxy composites increased the tensile property of SiO_2/epoxy composite [12]. Addition of silica formed a tribofilm on counter face under water lubrication which reduced a friction and

Please cite this article as: T. P. Sathishkumar, P. Navaneethakrishnan, and P. Maheskumar, "Thermal stability and tribological behaviors of tri-fillers reinforced epoxy hybrid composites," *Applied Science and Engineering Progress*, vol. 14, no. 4, pp. 727–737, Oct.–Dec. 2021, doi: 10.14416/j.asep.2021.08.002.

wear rate of epoxy composite [13]. The graphite and MoS_2 were used as solid lubricants in epoxy composites under water lubricant tribo test. Addition of graphite particle have improved a lubricant characteristic which reduced the friction up to 24% and also found that viscous property does not changes at higher temperature [14]. MoS_2 filled epoxy composite decreased the wear and friction coefficient which also increased heat dissipation under dry and wet running condition [15]. On comparing these two solid lubricants, graphite filler provided a better wear performance over MoS_2 due to oxidized of MoS_3 under sliding condition [16]. The coconut shell (Cocos nucifera) was used to prepare the natural filler for developing the polymer-based materials [17]. It consists of C (74.3%), O (21.9%), Si (0.2%), K (1.4%), S (0.5%), P (1.7%), and O/C (0.29%) [18].

The cashew nut shell filler was used a tribo filler for preparing the epoxy composites. Increasing the filler content was reducing the specific wear rate the less wear rate as found for composites containing maximum filler content of 25% [19]. Apart from adding filler with size and shape, functionally modified nanoparticle was increased the rate wear of polymer composite. The specific wear rate of epoxy was improved by incorporating the wax filled microcapsule and HDI filled microcapsule [20]. Compared to homogenous TiO_2, the graded TiO_2 was decreased wear and friction coefficient due to better interfacial bonding [21]. The wear rate had been controlled due to self-lubricating and self-healing [22]. The Taguchi's technique was used optimize the rice husk content in the composite's materials [23].

The filler reinforced polymer composites have great potential on tribological applications, but in certain cases, the high friction coefficient and wear rate of pure epoxy do not meet the requirements. In this work, tribological behaviour and thermal stability was studied in graphite, silica and coconut shell powder reinforced epoxy composite were studied. Optimization techniques were employed to obtain a minimum wear rate among various parameter such as applied load (10, 20 and 30 N), velocity (1, 1.5 and 2 m/s) and filler particle. The percentage contribution of each parameter and interactions were evaluated. And it's also aims to compare experimental value and predicted value obtained from regression equation.

2. Experimental Procedure

2.1 *Materials and preparation of composite*

The three elements namely coconut shell filler, silica filler and graphite fillers are used for preparing the epoxy composites. The coconut shell is part of a hard structural element in coconut fruit whish product the coconut white flesh and milk (i.e., liquid endosperm). The shells are collected from farmers, erode, Tamilnadu, India. Initially the outer coat of coconut fruits and white flesh (i.e., slid endosperm) were removed by manually remaining seed coat that is called coconut shells. Hereafter the shells outside surface were grinded to remove the coconut fibers and supporting elements. Then these shells were collectively dried in sun light for three day. After that the shells were cut into small pieces approximately 5 mm size and they were converted into filler from using grinding machine. The grinded coconut shell fillers were dried in sun light for 8 h and furthers dried in hot air woven for 3 h for removing the moisture content before the composite process. The laboratory used type graphite and silica fillers were purchased from the National Scientific Laboratory, Coimbatore, Tamil Nadu, India. The purity of these fillers is approximately 98%. The size of silica and graphite fillers are 0.1 and 1.16 mm.

2.2 *Thermal stability analysis*

Thermal decomposition patterns of virgin epoxy, fillers (silica, coconut and graphite), and SCG composites were carried out using thermo gravimetric analyzer (Berkline Elmer TGA/DTA 6300) from 30°C to 550°C temperature at a heating rate of 10°C/min. All samples of 10 mg were loaded in an aluminum crucible and tested in oxygen atmospheric condition. The TAG and DGA patterns were plotted percentage of weight of sample versus temperature. After decomposition, the weight of the residual was measured.

2.3 *Dry sliding parameter design by Taguchi's approach*

The Taguchi's method is commonly used approach for optimizing the design parameters for originally improving the quality of the product. Generally, the experimental procedures are more expensive and time

consuming. Then it should need to reduce the number of experiments for achieving the design objectives. For preliminary experiments plan, the three factors at three levels were planned by Taguchi's design approach shown in Table 1. It shows the three independent factors such as applied load (P), sliding speed (V) and weight fraction of fillers (%) in the SCG composites, and the range of each variables could directly influence the performance of dry sliding wear (i.e. wear rate, wear resistance and coefficient of friction) performance of all SCG composites. The chosen array was L27 (313) [23]. Table 2 shows the dry sliding wear of SCG reinforced epoxy composites.

Table 1: Parameters levels used in the experiments

Level	Applied Load, P(N)	Sliding Speed, V (m/s)	Weight Fraction of the Fillers, wt% (S+C+G)
1	10	1	10+10+10
2	20	2	10+10+20
3	30	3	10+10+30

S = Silica filler, C = Coconut filler and G = Graphite filler

Table 2: Results of dry sliding wear of SCG reinforced epoxy composites

Control Factors				Experimental Results			Statistical Results		
Number of Runs	Applied Load (P)	Sliding Speed (V)	Weigh of the Fillers (S+C+G)	Wear Rate (WR)	Wear Resistance (WRS)	Coefficient of Friction, (μ)	S/N Ratio for Wear Rate (db)	S/N Ratio for Wear Resistance (db)	S/N Ratio for COF (db)
	(N)	(m/s)	(wt%)	10^{-8} × (mm^3/N-m)	(N-m)/ mm^3				
1.	10	1	10+10+10	9.08	11009174.31	0.350	10.07	10061812	0.368
2.	10	1	10+10+20	11.67	8571428.57	0.410	11.16	8989072	0.389
3.	10	1	10+10+30	13.33	7500000.00	0.390	12.25	7916332	0.411
4.	10	1.5	10+10+10	10.83	9230769.23	0.410	10.02	10193423	0.445
5.	10	1.5	10+10+20	10.00	10000000.00	0.430	11.11	9120683	0.466
6.	10	1.5	10+10+30	11.67	8571428.57	0.450	12.20	8047943	0.488
7.	10	2	10+10+10	10.00	10000000.00	0.480	9.97	10325033	0.522
8.	10	2	10+10+20	10.83	9230769.23	0.610	11.06	9252293	0.543
9.	10	2	10+10+30	14.17	7058823.53	0.630	12.15	8179553	0.565
10.	20	1	10+10+10	8.75	11428571.43	0.415	8.85	11297192	0.437
11.	20	1	10+10+20	10.00	10000000.00	0.495	9.94	10224452	0.459
12.	20	1	10+10+30	10.42	9600000.00	0.530	11.04	9151712	0.480
13.	20	1.5	10+10+10	8.75	11428571.43	0.580	8.80	11428803	0.514
14.	20	1.5	10+10+20	9.17	10909090.91	0.495	9.89	10356063	0.536
15.	20	1.5	10+10+30	10.83	9230769.23	0.475	10.99	9283323	0.557
16.	20	2	10+10+10	8.33	12000000.00	0.565	8.75	11560413	0.591
17.	20	2	10+10+20	9.58	10434782.61	0.645	9.84	10487673	0.613
18.	20	2	10+10+30	10.00	10000000.00	0.690	10.94	9414933	0.635
19.	30	1	10+10+10	8.06	12413793.10	0.530	7.64	12532572	0.506
20.	30	1	10+10+20	8.89	11250000.00	0.450	8.73	11459832	0.528
21.	30	1	10+10+30	9.72	10285714.29	0.610	9.82	10387092	0.550
22.	30	1.5	10+10+10	8.61	11612903.23	0.660	7.59	12664183	0.583
23.	30	1.5	10+10+20	10.28	9729729.73	0.523	8.68	11591443	0.605
24.	30	1.5	10+10+30	8.06	12413793.10	0.687	9.77	10518703	0.627
25.	30	2	10+10+10	7.22	13846153.85	0.720	7.54	12795793	0.660
26.	30	2	10+10+20	7.78	12857142.86	0.587	8.63	11723053	0.682
27.	30	2	10+10+30	11.11	9000000.00	0.640	9.72	10650313	0.704

(S= Silica, C = Coconut, G = Graphite)

2.4 *Wear and friction testing procedure*

The tribological properties of epoxy composite have been conducted as per ASTM G99 in pin on disc tribometer. An alumina disc has been chosen as counter surface. The samples were firmly attached perpendicular to disc on sample holder and load applied with help of lever mechanism. The parameter like velocity and sliding distance has been adjusted by computerized control. The test was carried out in dry condition for 1.2 km with different load and velocity. Before holding, a specimen was weighed on high precision (0.1 mg) weighing machine and value was tabulated. At end of test weight of sample was weighed and mass losses of samples were calculated. The wear rate has been calculated with below Equation (1) [24], [25].

$$Wear\ rate = \frac{\Delta m}{F_N L} \quad (1)$$

Where Δm is mass loss during test (mg), F_N is normal load (N) and L is sliding distance (km).

2.5 *Morphology analysis*

The morphology of particle and topography of worn-out surface formed under different load and velocity were examined by taking photography on scanning electron microscope. The topography was analyzed on wear track region by thin layered gold coating.

3 Results and Discussion

3.1 *Thermal stability*

The thermal stability of composites was determined by using thermo-gravimetric analyzer. The TGA curves of pure epoxy and the SCG composites with different SCG content are shown in Figure 1. It is observed that pure graphite exhibits very high thermal stability with only 1.6% total weight loss up to 800°C. On the other hand, both pure epoxy and the composites shows thermal degradation at much lower temperatures and significant weight loss with temperature. The onset and the end set of thermal degradation temperature were determined from the intersection of two tangents. The TGA values of pure epoxy and its composites indicate that the thermal stability of the pure epoxy was enhanced by the incorporation of graphite particles. For

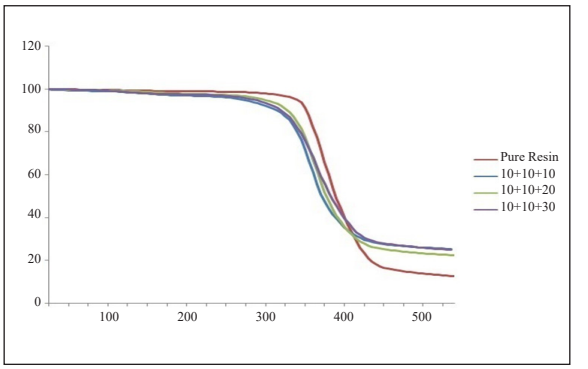

Figure 1: TGA of pure epoxy and the SCG composites.

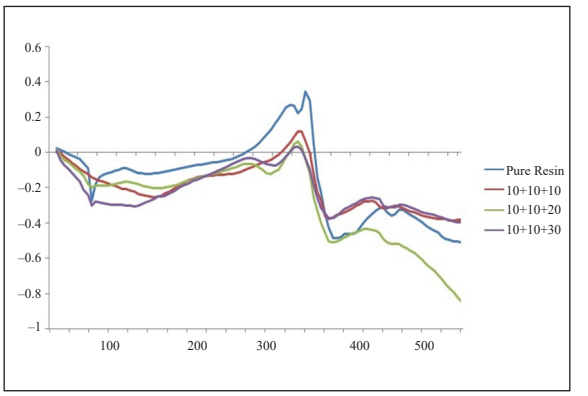

Figure 2: DSC of pure epoxy and the SCG composites.

pure epoxy, the onset temperature is 357°C, while for the SCG composites it starts to decrease from 338°C for 10 wt% SCG composites and 342°C for 20 wt% SCG composites 340°C for 30 wt% SCG composites. The incorporation of silica, CSP and graphite particles in pure epoxy matrix decreases the decomposition temperature of pure epoxy. The SCG composites shows higher char content and reduced weight loss at 400°C as the graphite content increases. Therefore, the incorporation of the graphite platelet resulted improvement in thermal stability. The improvement of thermal stability due to the addition of nanoparticles has also been reported for other composites [26], [27]. The influence of graphite on the curing of kinetics was confirmed by DSC analysis. Figure 2 shows the DSC results for various concentrations of SCG concentrations. It can be seen that an increase in the graphite concentration leads to decrease in the total heat of reaction.

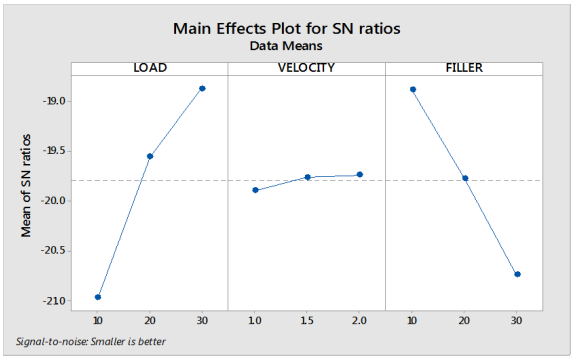

Figure 3: Mean effects plot of means -wear rate.

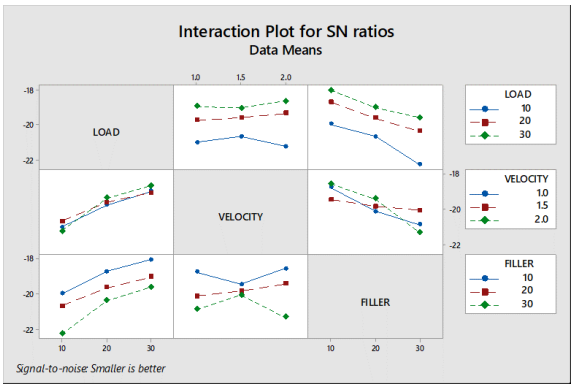

Figure 4: Interaction plots of wear rate.

3.2 *Dry sliding wear and friction test*

3.2.1 Effect of parameters on wear rate

The signal-to-noise (S/N) response for wear resistance is shown in Table 3. It is the average of S/N ratio at corresponding level. An optimal condition can be obtained at input parameter with highest S/N ratio. It observes that load at 30 N, velocity at 2 m/s and filler content at 10 wt% Gr provided an optimal condition of wear rate. Also ranking provided in this table reveled that normal load has significant effect on wear rate and followed by weight fraction of filler and sliding velocity. The graphical representation oof mean effective plot of SN ratio and wear resistance has been shown in Figure 3. From this figure, the wear rate increased with increasing the load and velocity whereas increasing the filler content leads to decrease in wear rate. The interaction of input parameters has been shown in Figure 4. Table 4 shows the results of the ANOVA of wear rate for epoxy composite. The analysis done at level of significance of 5% i.e., level of confidence 95%. The last column indicates percentage of contribution (*p*-value). If percentage of contribution reduced, then it has significant contribution on wear rate. Here, load (0.03) and velocity (0.006) have significant contribution and interaction between load x filler content (0.644) and velocity x filler content (0.313) has greater influence on wear rate. The equal ratio of fillers content in the epoxy composites showed lesser wear rate.

Table 3: Signal to noise response for wear rate

Level	Applied Load, P, (N)	Sliding Speed, (V), m/s	Weigh of the Fillers, %, (S+C+G)
1	–20.97	–19.89	–18.88*
2	–19.56	–19.76	–19.77
3	–18.87*	–19.74*	–20.75
Delta	2.1	0.15	1.86
Rank	1	3	2

Table 4: Analysis of variance for wear rate

Source	DOF	Sequential Sumof Square	Adjacent Sum of Square	Adjacent Mean Square	F-Test	*p*-value
Load	2	28.27	28.271	14.13	13.49	0.003
Velocity	2	0.164	0.1648	0.08	0.08	0.925
Filler content	2	21.60	21.608	10.8	10.31	0.006
Load × Velocity	4	1.291	1.2916	0.32	0.31	0.865
Load × Filler content	4	2.713	2.7131	0.67	0.65	0.644
Velocity × Filler content	4	5.927	5.9272	1.48	1.41	0.313
Error	8	8.384	8.3848	1.04		
Total	26	68.36				

3.2.2 Effect of wear resistance

The S/N noise response for wear resistance is shown in Table 5, which shows the average of S/N ratio at corresponding level. An optimal condition can be obtained at input parameter with highest S/N ratio. From this table it observed that 30 N of load, 2 m/s of velocity and 10 wt% Gr filled epoxy composite provided an optimal value of wear resistance. The ranking provided in this table indicates that applied load has significant effect on wear resistance and

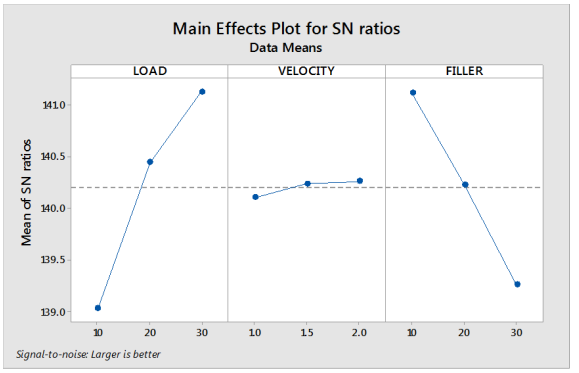

Figure 5: Mean effects plot of means wear resistance.

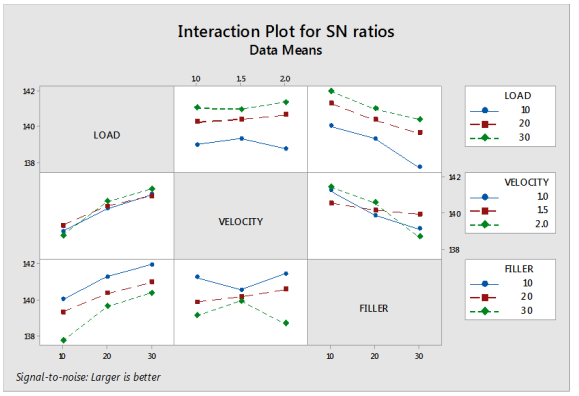

Figure 6: Interaction plots of wear resistance.

followed by weight fraction of filler and sliding velocity. The graphical representation of mean effective plot of S/N ratio and wear resistance has been shown in Figure 5. In this figure, the wear resistance is increased with increasing in load and velocity whereas increase in filler content is leads to decrease in wear resistance. Figure 6 shows the interaction plots between variables. The interaction of load and velocity was increasing the wear resistance when composite containing the 10% of Gr filler. Table 6 shows the results of the ANOVA for wear resistance of epoxy composite. The analysis done at level of significance of 5% i.e., level of confidence 95%. The last column indicates percentage of contribution (*p*-value). If percentage of contribution reduced, then it has significant contribution on wear resistance. Here, load (0.005) and velocity (0.013) have significant contribution and interaction between load x velocity (0.917) and velocity x filler content (0.382) has greater influence on wear resistance.

Table 5: Signal to noise response for wear resistance

Level	Applied Load, P	Sliding Speed, (V)	Weight Fraction of the Fillers, wt, (S+C+G)
	N	m/s	%
1	139	140.1	141.1
2	140.1	140.2	140.2
3	141.4*	140.3*	139.3
Delta	2.1	0.2	1.9
Rank	1	3	2

Table 6: Analysis of variance for wear resistance

Source	DOF	Sequential Sum of Square	Adjacent Sum of Square	Adjacent Mean Square	F-Test	*p*-value
Load	2	2.80E+13	2.80E+13	1.40E+13	10.76	0.005
Velocity	2	3.13E+11	3.13E+11	1.56E+11	0.12	0.888
Filler content	2	2.07E+13	2.07E+13	1.04E+13	7.95	0.013
Load× Velocity	4	1.17E+12	1.17E+12	2.93E+11	0.22	0.917
Load× Filler content	4	6.40E+11	6.40E+11	1.60E+11	0.12	0.97
Velocity× Filler content	4	6.24E+12	6.24E+12	1.56E+12	1.2	0.382
Error	8	1.04E+13	1.04E+13	1.30E+12		
Total	26	6.75E+13				

3.2.3 Effect of parameters on friction coefficient

Table 7 represents signal-to-noise response for friction coefficient of epoxy composites and observed that input parameter with highest S/N ratio provides an optimal value with minimum variance. The optimal conditions are obtained at 30N of load, velocity of 2 m/s and 30 wt% filled graphite content. As ranking provided in this table, it is observed that sliding speed has greater influence on friction coefficient than load and weigh of fillers. However, the level difference between the variables were very minimum. The graphical representation of S/N ratio and effect of control parameters are shown in Figure 7. The coefficient of friction is increasing with increase in load and velocity. The mid line indicates mean S/N ratio. The similar

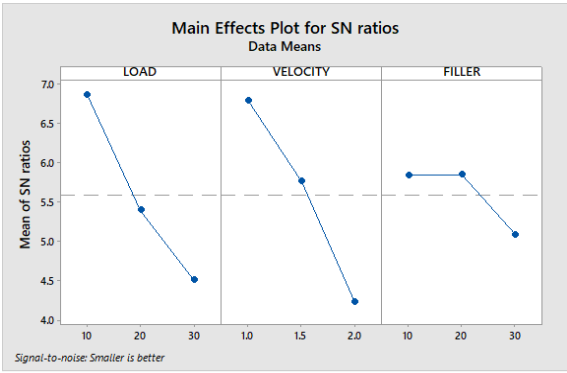

Figure 7: Mean effects plot of means - coefficient of friction.

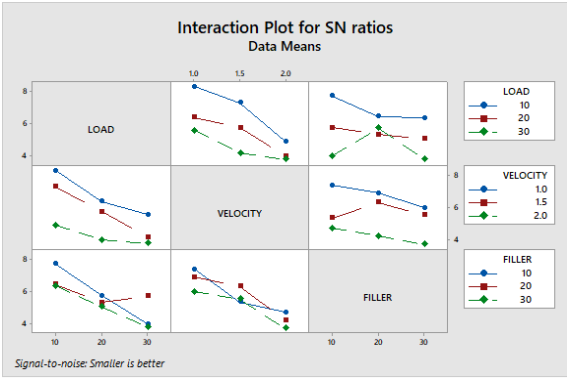

Figure 8: Interaction plots of coefficient of friction.

friction coefficient was observed on 10 and 20 wt% graphite filled epoxy composite. Further increase in graphite leads to increase in friction coefficient. The optimal parameter is found on 10N of applied load, 1m/s of sliding speed and 20 wt% graphite filled epoxy composites. The interaction plots of coefficient of friction have been shown in Figure 8. Table 8 shows Analysis of Variance (ANOVA) results on coefficient of friction. The ANOVA is done for a level of confidence of 95% (level of significance of 5%). The seventh column of table indicates percentage of contribution (P). If P value of parameter decreases, that parameter has significant contribution on result. Here, load and velocity (0.001) have significant contribution on friction coefficient. Conversely, interaction of load x velocity (0.392) and load x filler content (0.093) has significant contribution on friction coefficient while other parameter and interaction has lower contribution on coefficient of friction.

Table 7: Signal to noise response for coefficient of friction

Level	Applied Load, P, (N)	Sliding Speed, (V), m/s	Weigh of the Fillers, %, (S+C+G)
1	6.859	6.783	5.838
2	5.395	5.757	5.843
3	4.512*	4.226*	5.085
Delta	2.348	2.557	0.758
Rank	2	1	3

Table 8: Analysis of variance for coefficient of friction

Source	DOF	Sequential Sum of Square	Adjacent Sum of Square	Adjacent Mean Square	F-Test	*p*-value
Load	2	0.08719	0.08719	0.043593	17.02	0.001
Velocity	2	0.1088	0.1088	0.0544	21.23	0.001
Filler content	2	0.01356	0.01356	0.006781	2.65	0.131
Load× Velocity	4	0.01199	0.01199	0.002997	1.17	0.392
Load× Filler content	4	0.02976	0.02976	0.007441	2.9	0.093
Veloc-ity× Filler content	4	0.01046	0.01046	0.002614	1.02	0.452
Error	8	0.0205	0.0205	0.002562		
Total	26	0.28225				

3.2.4 Multiple linear regression model

The multiple regression model has been developed using "MINITAB 18" statistical software. This equation provides a relationship between an actual value and predicted value by fitting a linear equation to the observed data. Among various regression equation multiple linear models was used for tribo studies. The regression equation for friction coefficient, wear rate and resistance were founded as follows.

$$\textit{Wear resistance} = 9635951 + 123538\ \textit{Load} + 263221\ \textit{Velocity} - 107274\ \textit{Filler} \quad (2)$$

$$\textit{Wear rate} = 10.286 - 0.1215\ \textit{Load} - 0.099\ \textit{Velocity} + 0.1093\ \textit{Filler} \quad (3)$$

Coefficient of friction = 0.1223 + 0.00693 *Load* + 0.1541 *Velocity* + 0.00218 *Filler* (4)

From Equation (2), the negative sign indicates that wear resistance decreases with increase in filler content whereas wear rate decreased by increasing the load and velocity as shown in Equation (3). For coefficient of friction, addition of load, velocity and filler tends to increase in friction coefficient which is revealed in Equation (4).

3.2.5 Confirmation test

The conformation results for coefficient of friction, wear rate and resistance has been shown in Table 9. The final step of DOE approach is to verify the estimated results with prediction value obtained from regression equation. The conformation test is performed to optimal parameters of A3B3C1 (i.e., A3 = 30 N, B3 = 2 m/s and C1 = 10% Gr filler). The error percentage of experimental and prediction value observed to be 5.12, 4.34 and 7.58% for friction coefficient, wear rate and resistance. The increase in number of measurements may tends to decrease in error. This validates the development of mathematical model for predicting the measure of performance-based knowledge of input parameters.

Table 9: Conformation test result for output parameters

	Optimal Parameter Condition	Experimental Value	Prediction Value	Error (%)
Coefficient of friction	A3B3C2 (30 N, 2 m/s and 20% Gr)	0.41	0.389	5.12
Wear rate (10^{-8}) (mm^3/N-m))	A3B3C1 (30 N, 2 m/s and 10% Gr)	7.22	7.54	4.34
Wear resistance ((N-m)/ mm^3)		13846153.85	12795793	7.58

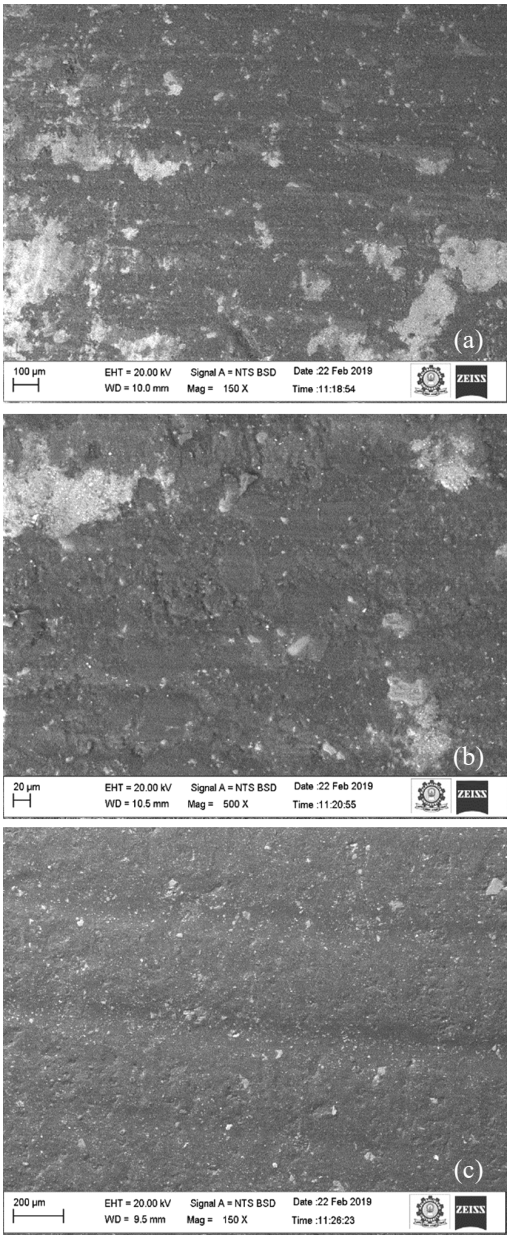

Figure 9: SEM micrographs of SCG composite: (a) SCG = 10 w% of graphite; (b) SCG = 20 w% of graphite and (c) SCG = 30 w% of graphite.

3.3 *Morphology of worm surfaces*

The wear mechanism on worn-out surface has been examined using Scanning Electron Microscopic (SEM) image shown in Figure 9(a)–(c). It shows that the dispersion of the silica particles with epoxy resin in uniform than that of coconut shell powder and Graphite particles with during the specimen preparation process. Interfacial bonding between the matrix and fillers was found better. The wear resistance of the composites will be enhanced by the effective transfer of the applied load from the matrix to the reinforcement materials

[28], [29]. The formation of wear track on the worn-out surface was ups and downs at less Gr filler content [Figure 9(a)]. Increasing the Gr content, the wear track was shown smooth and the formation of thin film on the surface is very less [Figure 9(c)]. The increasing Gr filler content was increasing the heat transfer rate of the composites pin during the tribo test.

4 Conclusions

The thermal stability and tribological behaviour were studied on tri-fillers reinforced epoxy hybrid composites and the conclusion are obtained. The dry wear tribological test was performed on the tri-fillers reinforced epoxy composites by varying sliding speed, applied load and filler concentration using pin-on-disk method. The design of experiments was planned based on the Taguchi's techniques and considering list of experiments by L27 orthogonal array. The increasing the applied load and sliding velocity were increasing the wear resistance and decreasing the wear rate, but the increasing the Gr content was increased the coefficient of wear. Hence optimization process, an optimal parameter found as 30 N of load, 2 m/s of sliding velocity and 10 wt% of graphite for wear rate and resistance. Similarly, for coefficient of friction 10 N of load, 1 m/s of sliding velocity and 10 wt% of graphite. By ANOVA table, applied load and velocity has lower influence (0.1%) on friction coefficient whereas filler content has greater influence (13.1%) on friction coefficient. On other hand, wear rate is significantly depending on velocity (92.5%) and lower influence on filler content (0.6%) and normal load (0.3%). The conformation test shows error percentage between experimental and predicted values. The obtained errors are 5.12, 4.34 and 7.58% for frictional coefficient, wear rate and resistance. The morphology of worn-out surface showed that the formation of wear track and thin film formation was found less in 30 N of load, 2 m/s of sliding velocity and 30 wt% of graphite.

Reference

[1] S. M. Rangappa, S. Siengchin, and H. N. Dhakal, "Green-composites: Ecofriendly and sustainability," *Applied Science and Engineering Progress*, vol. 13, no. 3, pp. 183–184, 2020, doi: 10.14416/j.asep.2020.06.001.

[2] M. Jawaid and S. Siengchin, "Hybrid composites: A versatile material for future," *Applied Science and Engineering Progress*, vol. 12, no.4, p. 223, 2019, doi:10.14416/j.asep.2019.09.002.

[3] S. M. K. Thiagamani, S. Krishnasamy, and S. Siengchin, "Challenges of biodegradable polymers: An environmental perspective," *Applied Science and Engineering Progress*, vol. 12, no. 3, p. 149, 2019, doi:10.14416/j.asep.2019.03.002.

[4] M. Zamanian, M. Mortezaei, B. Salehnia, and J. E. Jam, "Fracture toughness of epoxy polymer modified with nanosilica particles: Particle size effect," *Engineering Fracture Mechanics*, vol. 97, pp. 193–206, 2013, doi:10.1016/j.engfracmech.2012.10.027.

[5] H.-Y. Liu, G.-T. Wang, Y.-W. Mai, and Y. Zeng, "On fracture toughness of nano-particle modified epoxy," *Composites Part B: Engineering*, vol. 42, no. 8, pp. 2170–2175, 2011, doi: 10.1016/j.compositesb. 2011.05.014.

[6] R. V. Kurahattia, A. O. Surendranathan, A. V. R. Kumar, C. S. Wadageri, V. Auradi, and S. A. Kori, "Dry sliding wear behaviour of epoxy reinforced with nanoZrO_2 particles," *Procedia Materials Science*, vol. 5, pp. 274–280, 2014, doi: 10.1016/j.mspro.2014.07.267.

[7] Z. Zhang, C. Breidt, L. Chang, F. Haupert, and K. Friedrich, "Enhancement of the wear resistance of epoxy: Short carbon fibre, graphite, PTFE and nano-TiO_2," *Composites: Part A*, vol. 35, pp. 1385–1392, 2004, doi:10.1016/j.compositesa.2004.05.005.

[8] F. Li, K.-A. Hu, J.-L Li, and B.-Y. Zhao, "The friction and wear characteristics of nanometer ZnO filled polytetrafluoroethylene," *Wear*, vol. 249, pp. 877–882, 2002, doi: 10.1016/S0043-1648(01)00816-X.

[9] J. Xu, H. Yan, and D. Gu, "Friction and wear behavior of polytetrafluoroethene composites filled with Ti_3SiC_2," *Materials and Design*, vol. 61, pp. 270–274, 2014, doi: 10.1016/j.matdes.2014.04.069.

[10] B. Wetzel, F. Haupert, and M. Q. Zhang, "Epoxy nanocomposites with high mechanical and tribological performance," *Composites Science and Technology*, vol. 63, pp. 2055–2067, 2003, doi: 10.1016/S0266-3538(03)00115-5.

[11] Y. L. Liang and R. A. Pearson, "Toughening mechanisms in epoxy–silica nanocomposites

(ESNs)," *Polymer*, vol. 50, pp. 4895–4905, 2009, doi: 10.1016/j.polymer.2009.08.014.

[12] J. Abenojar, J. Tutor, Y. Ballesteros, J. C. del Real, and M. A. Martínez, "Erosion-wear, mechanical and thermal properties of silica filled epoxy nanocomposites," *Composites: Part B*, vol. 120, pp. 42–53, 2017, doi: 10.1016/j.compositesb.2017.03.047.

[13] M. Zappalorto, A. Pontefisso, A. Fabrizi, and M. Quaresimin, "Mechanical behaviour of epoxy/silica nanocomposites: Experiments and modeling," *Composites: Part A*, vol. 72, pp. 58–64, 2015, doi: 10.1016/j.compositesa.2015.01.027.

[14] C. P. Gao, G. F. Guo, F. Y. Zhao, T. M. Wang, B. Jim, B. Wetzel, G. Zhang, and Q. H. Wang, "Tribological behaviors of epoxy composites under water lubrication conditions," *Tribology International*, vol. 95, pp. 333–341, 2016, doi: 10.1016/j.triboint.2015.11.041.

[15] C.-G. Lee, Y.-J. Hwang, Y.-M. Choi, J.-K. Lee, C. Choi, and J.-M. Oh, "A study on the tribological characteristics of graphite nano lubricants," *International Journal of Precision Engineering and Manufacturing*, vol. 10, pp. 85–90, 2009, doi: 10.1007/S12541-009-0013-4.

[16] B. B. Difallah, M. Kharrat, M. Dammak, and G. Monteil, "Improvement in the tribological performance of polycarbonate via the incorporation of molybdenum disulfide particles," *Tribology Transactions*, vol. 57, no. 5, pp. 806–813, 2014, doi: 10.1080/10402004.2014.913751.

[17] H.-J. Zhang, Z.-Z. Zhang, and F. Guo, "Studies of the influence of graphite and MoS_2 on the tribological behaviors of hybrid PTFE/Nomex fabric composite," *Tribology Transactions*, vol. 54, no. 3, pp. 417–423. doi: 10.1080/10402004.2011.553027.

[18] C. D. Liyanage and M. Pieris, "A physico-chemical analysis of coconut shell powder," *Procedia Chemistry*, vol. 16, pp. 222–228, 2015, doi: 10.1016/j.proche.2015.12.045.

[19] A. K. Bledzki, A. A. Mamun, and J. Volk, "Barley husk and coconut shell reinforced polypropylene composites: The effect of fibre physical, chemical and surface properties," *Composites Science and Technology*, vol. 70, pp. 840–846, 2010, doi:10.1016/j.compscitech.2010.01.022.

[20] N. W. Khun, H. Zhang, D. W. Sun, and J. L. Yang, "Tribological behaviors of binary and ternary epoxy composites functionalized with different microcapsules and reinforced by short carbon fibers," *Wear*, vol. 350–351, pp. 89–98, 2016, doi:10.1016/j.wear.2016.01.007.

[21] Siddhartha, A. Patnaik, and A. D. Bhatt, "Mechanical and dry sliding wear characterization of epoxy–TiO_2 particulate filled functionally graded composites materials using Taguchi design of experiment," *Materials & Design*, vol. 32, no. 2, pp. 615–627, 2011, doi:10.1016/j.matdes.2010.08.011.

[22] N. W. Khun, D. W. Sun, M. X. Huang, J. L. Yang, and C. Y. Yue, "Wear resistant epoxy composites with diisocyanate-based self-healing functionality," *Wear*, vol. 313, pp. 19–28, 2014, doi: 10.1016/j.wear.2014.02.011.

[23] L.-C. Tang, H. Zhang, J.-H. Han, X.-P. Wu, and Z. Zhang, "Fracture mechanisms of epoxy filled with ozone functionalized multi-wall carbon nanotubes," *Composites Science and Technology*, vol. 72, no. 1, pp. 7–13, 2011, doi:10.1016/j.compscitech.2011.07.016.

[24] J. Zhua, L. Mab, and R. Dwyer-Joyce, "Friction and wear behaviours of self-lubricating peek composites for articulating pin joints," *Tirbology International*, vol. 149, p. 105741, 2019.

[25] A. Kurdia, W. H. Kana, and L. Chang, "Tribological behaviour of high performance polymers and polymer composites at elevated temperature," *Tirbology International*, vol. 130, pp. 94–105, 2019.

[26] A. Verma, L. Budiyal, and S. M. Rangappa, and S. Siengchin, "Processing and characterization analysis of pyrolyzed oil rubber (from waste tires) -epoxy polymer blend composite for lightweight structures and coatings applications," *Polymer Engineering & Science*, vol. 59, no. 10, pp. 2041–2051, 2019.

[27] A. Verma, K. Baurai, S. M. Rangappa, and S. Siengchin, "Mechanical, microstructural, and thermal characterization insights of pyrolyzed carbon black from waste tires reinforced epoxy nanocomposites for coating application," *Polymer Composites*, vol. 41, no. 1, pp. 338–349, 2020.

[28] K. N. Bharath, P. Madhu, T. G. Y. Gowda, A. Verma, S. M. Rangappa, and S. Siengchin, "A novel approach for development of printed circuit board from biofiber based composites," *Polymer*

Composites, vol. 41, no.11, pp. 4550–4558, 2020.
[29] M. K. Marichelvam, P Manimaran, A. Verma, S. M. Rangappa, S. Siengchin, K. Kandakodeeswaran, and M. Geetha, "A novel palm sheath and sugarcane bagasse fiber based hybrid composites for automotive applications: An experimental approach," *Polymer Composites*, vol. 42, no. 1, pp. 512–521, 2021.